

TRIBOLOGICAL PERFORMANCE OF Ni-W/PTFE COMPOSITE COATING VIA PULSE ELECTRODEPOSITION

by

**Arif KARADAG^{a*}, Erhan DURU^b, Mehmet UYSAL^b,
Hatem AKBULUT^{b,c}, and Aslan COBAN^d**

^a Department of Manufacturing Engineering, Graduate Education Institute,
Sakarya University of Applied Sciences, Sakarya, Turkey

^b Department of Metallurgy and Materials Engineering, Faculty of Engineering,
Sakarya University, Sakarya, Turkey

^c Central Research Laboratory (SARGEM), Esentepe Campus, Sakarya, Turkey

^d Mechanical Engineering Department, Faculty of Technology,
Sakarya University of Applied Sciences, Sakarya, Turkey

Original scientific paper

<https://doi.org/10.2298/TSCI2204885K>

The Ni-W/PTFE co-depositions were successfully prepared on steel via pulse electrodeposition methods. Electrodeposition was performed by dispersing 5-20 g/L PTFE particles from Ni-Watt bath. The surface morphology, phase analyses, crystallite size, distortion and hardness of the samples were characterized by SEM, XRD, and Vicker's microhardness tester. The friction coefficient of the coatings were carried out using CSM microtester. As increasing with the concentration of the PTFE in the solution, the wear resistance properties of the co-depositions were increased. These experimental results determined that the PTFE concentration of 15 g/L in the electrolyte was the optimum content to obtain the best micro-structure and wear performance.

Key words: pulse plating, Ni-W/PTFE electrodeposition, microhardness, tribological behavior

Introduction

The cost of damages caused by corrosion and wear in the material is serious. In recent years, one of the focal points of materials engineering is the reduction of costs due to wear and corrosion [1, 2]. There are many ways to increase the wear and corrosion resistance of the material surface. One of them is to apply a metallic coating to the surface of the material [3, 4]. Although there are many metallic coating methods today, the electrodeposition method is one step ahead thanks to its high efficiency and practicality in industrial applications [5].

Among electrodeposition, the most popular coatings are Ni-based coatings. In addition Ni element, it is also possible to carry out binary or ternary alloy coatings with the reinforcement of alloying elements such as P, Mo, W, and B [6-9]. It is possible to produce high performance Ni-Watt (Ni-W) coatings, especially with reinforcing elements such as tungsten, with superior mechanical and physical properties and high melting temperatures. Thanks to the high wear resistance, chemical stability and superior mechanical properties of Ni-W coatings, it can

* Corresponding author, e-mail: a.karadag@alparslan.edu.tr

find application opportunities in many industrial areas. In addition, Ni-W coatings have a more environmentally friendly side, especially when compared to hard chrome coatings [10-13].

Another research topic in recent years is the production and development of composite Ni-W coatings with the reinforcement of ceramic and polymer materials. It is well known that the chemical and physical properties of Ni-W plating will improve with these second-phases reinforcements. It was observed that the hardness and wear resistance of the coatings increased with ceramic particle reinforcement such as Al₂O₃, SiC, TiO₂, SiO₂, TiN [14-18]. With the reinforcement of materials such as MoS₂, Graphene oxide, PTFE, reduces the friction coefficient by adding self-lubricating properties to the coatings [19-22].

The hydrophobic and self-lubricating properties of PTFE will significantly improve the corrosion and wear resistance of Ni-W coatings. In this study, Ni-W-PTFE composite coatings containing PTFE at different concentrations were produced. The Ni-W coatings were reinforced with PTFE at different concentrations, their wear behavior was investigated and the optimum concentration was determined. We believe that this study can bring solutions to the problem of wear and corrosion, especially in oil exploration and drilling equipment, transportation of oil and corrosive liquids.

Experimental methods

In this study, experiments were carried out on low carbon steel (St 37) substrate with dimensions of 30 mm × 20 mm × 5 mm. Before the coating process, the substrate material has been subjected to several pre-treatments. The surface of the steel substrate was first sanded, then treated in alkaline cleaning baths, and finally activated in an acidic bath (50 ml HCl + 50 ml distilled H₂O). The baths set up for the coating consist of NiSO₄, Na₂WO₄, Na₃C₆H₅O₇, NH₄Cl, and NaBr. A composite coating bath was established by adding a second solution containing PTFE at different concentrations to the coating baths. The CTAB was added as a surfactant to the second solution containing PTFE. The chemical amounts and operating conditions of the coating bath are given in tab. 1.

Table 1. Composition of bath and deposition parameters

Chemicals concentration		Operating conditions	
NiSO ₄ ·7H ₂ O	16 g/L	pH	8.5
Na ₂ WO ₄ ·2H ₂ O	46 g/L	Temperature [°C]	75
Na ₃ C ₆ H ₅ O ₇ ·2H ₂ O	147 g/L	Time [min]	45
NH ₄ Cl	25 g/L	Current density [Adm ⁻²]	10
NaBr	16 g/L	<i>t</i> _{on} - <i>t</i> _{off} [ms]	50-50
CTAB	0.5 g/L	Agitation rate [rpm]	150
PTFE particles	5, 10, 15, 20 g/L		

The surface structure and PTFE distribution of the samples fabricated at different PTFE content were investigated by SEM. The phase structure of the coatings was determined by the XRD method using CuK_α radiation at a wavelength of 1.54 Å. Using the data obtained as a result of XRD analysis, the crystal size and lattice distortion of the coatings at different PTFE concentrations were calculated. The Debby-Sherrer method was used in these calculations, the method followed was explained in detail in our previous studies [19-24]. The hardness change in the coatings was determined by the nanohardness method. Five hardnesses were taken for each sample, and a 50 mN load was applied for 10 seconds in the hardness measurement. While

calculating the hardness values, the mean hardness and standard deviations were taken into account. Finally, wear tests were carried out to see the effect of PTFE concentration on the wear behavior. Wear tests were carried out in a dry environment at room temperature using the ball-on-disk method. Wear tests were carried out at a speed of 25 cm/s and under a load of 2 N over a distance of 500 m. Each test was repeated three times.

Results and discussion

The surface morphology of co-depositions prepared with different PTFE concentrations in the coating solution is given in fig. 1. In general, the surface of the co-depositions is without crack and has no defects. It can be observed that many PTFE are incorporated in Ni-W matrix during coating. Obviously, the PTFE amount incorporated into the matrix increased with adding PTFE concentration (from 5-15 g/L), but then significantly reduced with further increasing the content of PTFE in the bath. The increase of the PTFE amount in the nickel-tungsten matrix from 0-9.4 wt.% is related to PTFE content in the solution. With the further increase of the PTFE in the electrolyte, the amount of PTFE incorporated into matrix reduces due to the agglomeration of the PTFE result from poor wettability. The incorporating of PTFE using the pulse electrodeposition method can be related to the addition of PTFE on the cathode, as reported by Guglielmi's theory [23-25].

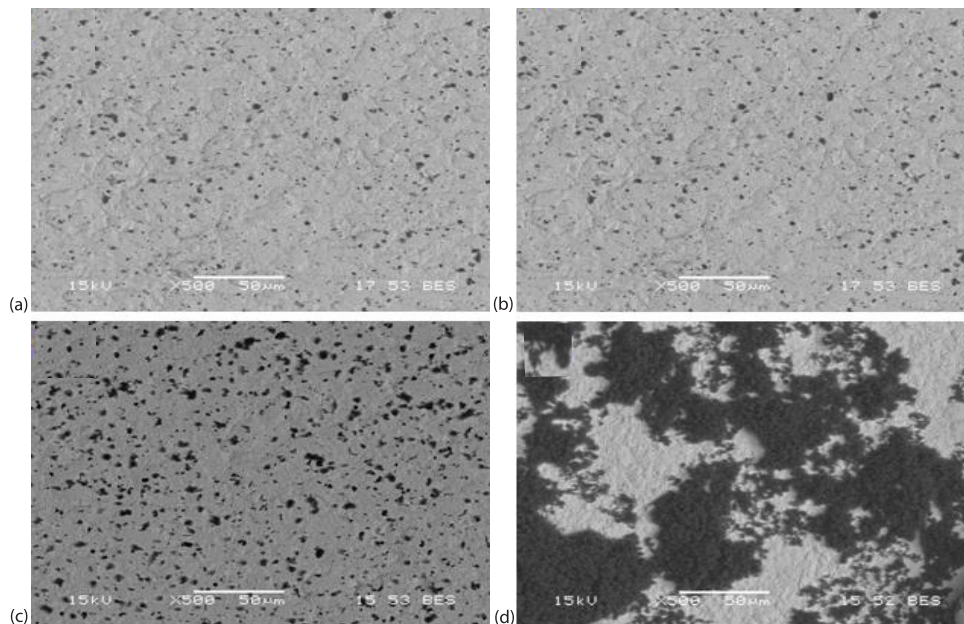


Figure 1. The SEM images of samples deposited at various PTFE content; (a) 5 g/L, (b) 10 g/L, (c) 15 g/L, and (d) 20 g/L

Figure 2(a) shows the XRD patterns of co-deposition prepared at various PTFE content in solution. The XRD spectrum of the Ni-W/PTFE co-deposition gives several peaks at 44.3°, 51.2°, and 77.1°, which correspond to the reflections of the Ni matrix phase (111), (200), and 220, respectively [24-26]. As seen in fig. 2(a), the peaks intensity increases with increasing PTFE content in the coating solution. The intensity of the diffraction (111) peaks of the samples is higher than that of the other co-depositions. This is due to the decreases in the crystallite size

of the coatings by the incorporating of PTFE into the plating bath. It can be determined that the crystallite size of Ni-W/PTFE composite coatings produced with different PTFE concentrations (5 g/L, 10 g/L, 15 g/L, and 20 g/L) is 17.59 nm, 14.21 nm, 9.44 nm, and 13.62 nm, respectively. The crystallite size of co-deposition firstly reduced with the increase of PTFE concentrations into solution from 5-15 g/L, then increased with further incorporating PTFE particles from 15-20 g/L. It indicates that the embedded PTFE have efficiently prohibits the growth of crystallites. The lattice distortions calculated according to the Scherrer equation are shown in fig. 2(b) at various PTFE content in the coating. With the increase of the PTFE particle ratio into bath, nickel the number of PTFE incorporated in the cage also increases. Thus, the compressive stress between the coating and the PTFE rises the degradation of the Ni lattice. This rise in Ni distortion may be due to the alloying of PTFE and W atoms in the coating. The crystallite size in presence of PTFE of 15 g/L was lower than that of other co-depositions suggesting that PTFE act as nucleating sites during electrodeposition. The PTFE incorporated to the electrolytic bath help nucleate the nickel, preventing grain growth, which result in decreasing crystal size and increasing the compactness of the nickel crystal [21, 27-29].

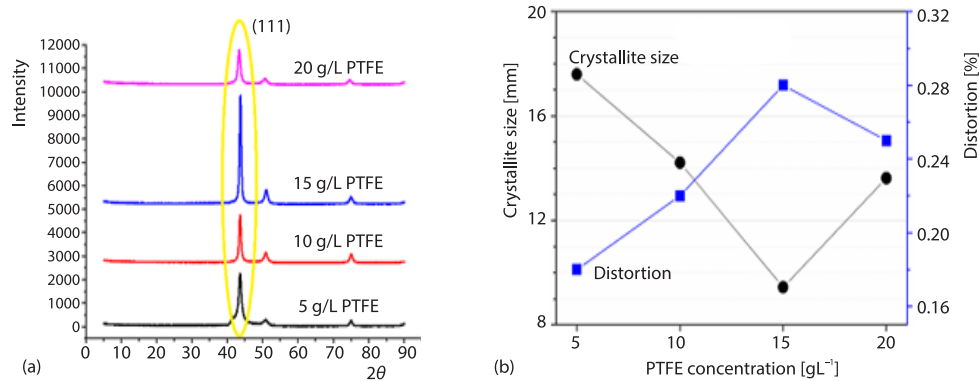


Figure 2. (a) the X-ray diffraction patterns and (b) lattice distortion and crystallite size of samples

Table 2 exhibits the hardness of co-depositions deposited at various concentrations of PTFE in the coating bath. Increasing the PTFE amount incorporated in the coating reduces the hardness of the matrix because of the soft of the PTFE lubricating [30]. Microhardness values for the samples electrodeposited with various PTFE concentration (5 g/L, 10 g/L, 15 g/L, 20 g/L) at constant current density of 10 A/dm² was 520 HV, 493 HV, 452 HV, and 417 HV, respectively. When the content of PTFE added solution is 20 g/L, corresponding to the much PTFE content into coating, the microhardness reaches a minimum value of 417 HV.

Table 2. The hardness measurement for samples produced at various concentrations

Sample	PTFE Concentration [gL ⁻¹]			
	5	10	15	20
Hardness (HV)	520 ±28	493 ±17	452 ±23	417 ±35

Figure 3 shows the wear rates and friction coefficients of samples produced at various PTFE content in the plating bath. The wear resistance of the co-deposition is related to the PTFE concentrations and roughness of the surface. The calculated wear rates for composite coatings deposited with 5 g/L, 10 g/L, 15 g/L, and 20 g/L were 3.03×10⁻⁷ mm³/Nm, 2.64·10⁻⁷ mm³/Nm,

$1.77 \cdot 10^{-7} \text{ mm}^3/\text{Nm}$, and $2.23 \cdot 10^{-7} \text{ mm}^3/\text{Nm}$, respectively. As shown in fig. 3(a), the wear rate decreases with increasing polymer particle content in the electrolyte, reaching its lowest value at a PTFE concentration of 15 g/L and then increasing at 20 g/L. This can be attributed to the agglomeration of PTFE particles into matrix deposition bath, poor interfaces between PTFE and the coating, and the lowest amount of PTFE incorporated in the Ni-W matrix. This study shows that Ni-W/PTFE composite coatings produced with a PTFE concentration of 15 g/L show the best wear resistance. Figure 3(b) exhibits for the coefficient of friction of PTFE reinforced composite coatings. As can be seen, increasing PTFE content in the solution caused a significant reduces in friction coefficient level. While friction coefficient of Ni-W alloy coated with electrolyte at 5 g/L PTFE concentration is around 0.42, this value decreases to 0.36 at 10 g/L PTFE concentration and 0.24 at 15 g/L PTFE concentration. At 20 g/L PTFE concentration, this value increases to 0.28. Moreover, as can be seen from fig. 3(b) is that the increase in PTFE concentration results in a more stable coefficient of friction of composite pavements at sliding distance. Allahyarzadeh *et al.* [31] reported that when there is plastic deformation, the matrix can carry the load and decreases stresses. According to this information, the increase in the load-carrying ratio of the co-deposition fabricated with 15 g/L PTFE incorporated to the solution compared to other samples can be due to the increase in the PTFE concentration [20, 29, 32, 33].

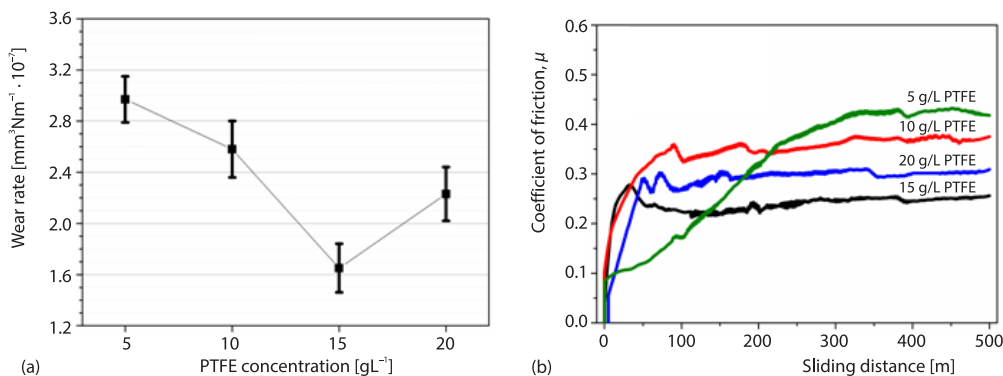


Figure 3. (a) Wear rate of coatings produced with different PTFE concentration and (b) coefficient of friction

The wear trace SEM images of Ni-W/PTFE co-deposition deposited at various PTFE content in the bath are displayed in fig. 4. The wear width of samples deposited at 5 g/L is also noticed that it is higher than that of other PTFE reinforced Ni-W co-depositions. For the sample produced at 5 g/L, its wear scar displays a large width of about 408 mm and is characterized by plastic deformation. On the contrary, for the sample fabricated at 15 g/L, the width of the wear scar is narrow, which is 182 mm, and the surface is smooth.

Figure 5 display SEM images (high magnification) of the wear tracks of samples deposited at various PTFE content. The wear track of sample fabricated at 5 g/L was observed high plastic deformation, which indicates the main wear mechanism is adhesive wear [34]. It was observed that as the PTFE concentration embedded into the coating increased, the plastic deformation that occurred at the interface decreased significantly. The furrows and cracks were observed on the Ni-W/PTFE composite coating's worn surface produced at 10 g/L, fig. 5(b), revealing fatigue wear. This suggests that the PTFE concentration of 10 g/L is low for load-carrying capacity. On the contrary, for the coating fabricated at 15 g/L, the width of the

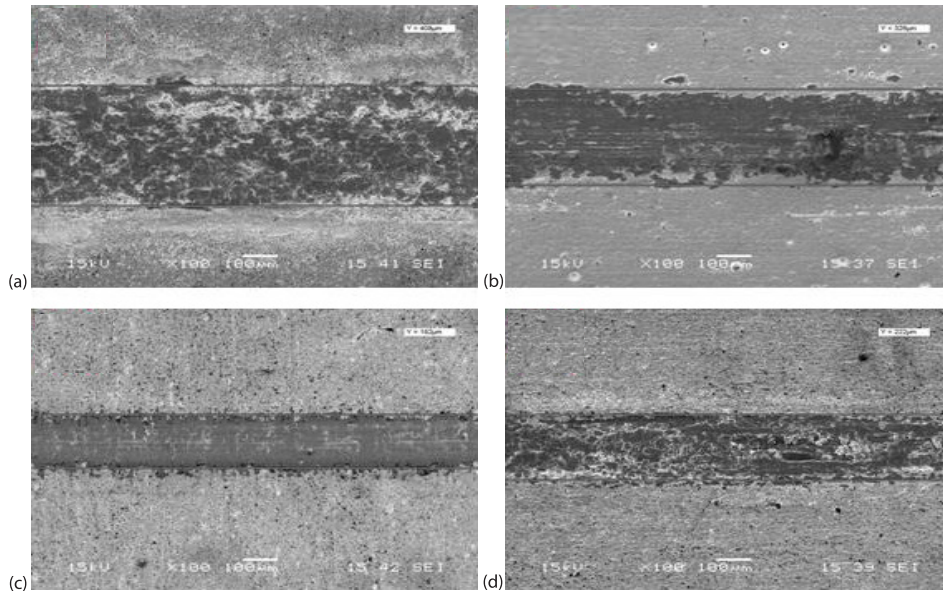


Figure 4. Wear trace images in $\times 100$ SEM image samples at various PTFE content; (a) 5 g/L ($Y = 408 \mu\text{m}$), (b) 10 g/L ($Y = 236 \mu\text{m}$), (c) 15 g/L ($Y = 182 \mu\text{m}$) and (d) 20 g/L ($Y = 222 \mu\text{m}$)

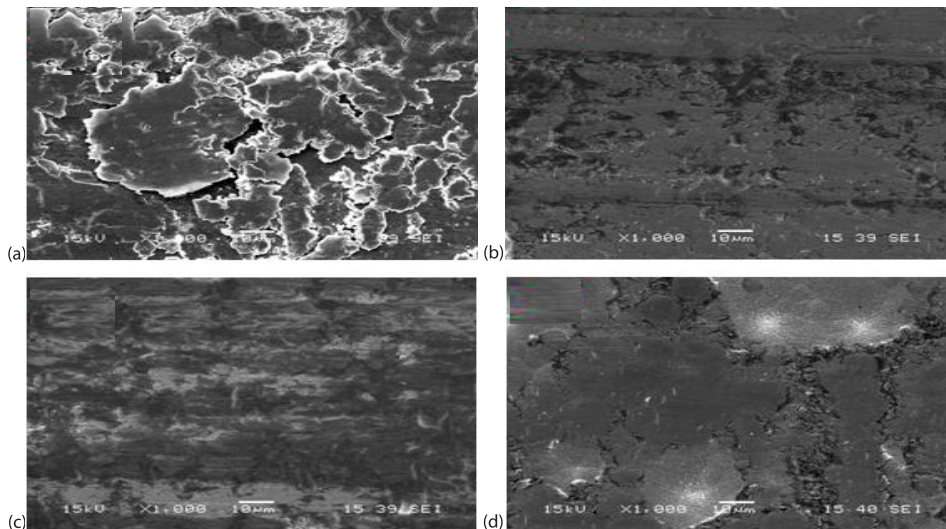


Figure 5. The SEM images of wear track of samples fabricated at various PTFE content; (a) 5 g/L and (b) 10 g/L, (c) 15 g/L, and (d) 20 g/L

wear track is narrow, and the appearance of the wear track is smooth with only a few ploughing, suggesting low abrasive wear. The homogeneous distribution of PTFE in the coating also ensures homogeneous load-bearing behavior due to plastic deformation decreases on the surface. Further increasing PTFE concentrations, the coating fabricated at 20 g/L was observed the severe delamination wear. As seen in fig. 5(d), the big parts of delamination and some micro-cracks are occurred on the wear track, increasing wear rate. This may be attributed to formed

surface roughness because of particle aggregation and poor hardness. The results suggested that an excellent surface protective layer formed at the interface between ball and coating, which is in agreement with the low friction coefficient for sample prepared at 15 g/L.

The 3-D topographies of the wear traces of the samples fabricated in the profilometer are exhibited in fig. 6. The surface roughness of coating is high and coating compatible with micro-structural results were observed for sample fabricated at 5 g/L. The PTFE reinforced coating fabricated at 15 g/L was observed a very smooth surface compared to other samples. Also, the scar depth and width of sample fabricated at 15 g/L are much smaller than the wear track other samples. This observation may be due to the fine-grained surface morphology of the coating and the uniform distribution of PTFE within the Ni coating. As for 20 g/L, it observed from fig. 6(d) that the width and depth of the wear marks on the coating surface also increase, and serious surface damage occurs on the surface. As a result, sample fabricated with a PTFE amount of 15 g/L shows the best tribological properties, which consistent with the wear test results.

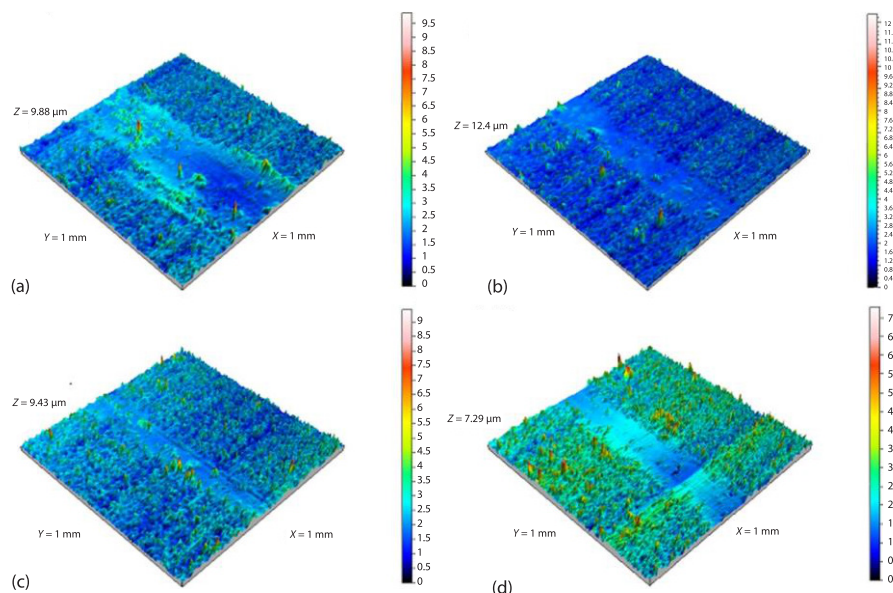


Figure 6. The 3-D profilometry results of samples; (a) 5 g/L, (b) 10 g/L, (c) 15 g/L, and (d) 20 g/L
 (for color image see journal web site)

Results

Surface morphology, hardness and friction properties of coatings deposited using the pulse electrodeposition were investigated. It was observed that the PTFE incorporated in the Na_2WO_4 coating were homogeneously distributed on the matrix and an intense without crack structure was obtained. The higher amount of PTFE increases the wt.% of sample deposited PTFE up to 15 g/L. The change in the content of incorporated PTFE resulted in changing the crystallite size, distortion hardenes and wear properties of the coating. Compared with other composite coating, sample prepared at 15 g/L has a lower crystallite size, surface roughness. The main wear mechanism for sample produced at 5 g/L was adhesive, while for sample produced at 15 g/L main wear mechanism was abrasion. For coating fabricated with a PTFE content of 15 g/L, wear track has smoother surfaces with less plastic deformation and without crack.

At 20 g/L, the wear mechanism transformed to severe plastic deformation and formation crack, which is result in delamination. Therefore, the wear rate increased but the friction increased. The co-deposition fabricated with a PTFE content of 15 g/L displayed the best wear performance than other composite coatings, and accordingly the lowest coefficient of friction.

Authorship contribution statement

Arif Karadag (<https://orcid.org/0000-0001-8077-8792>): Writing-Original Draft; Writing-Review and Editing; Visualization; Methodology; Conceptualization; Validation; Investigation.

Erhan Duru (<https://orcid.org/0000-0002-6205-6566>): Visualization; Writing-Review & Editing; Data Curation; Investigation; Formal analysis.

Mehmet Uysal (<https://orcid.org/0000-0002-9396-7450>): Writing-Review & Editing; Investigation; Methodology.

Hatem Akbulut (<https://orcid.org/0000-0002-6299-136X>): Supervision; Conceptualization; Resources; Writing-Review & Editing.

Aslan Coban (<https://orcid.org/0000-0001-5896-2964>): Funding acquisition; Project administration; Supervision; Writing-Review & Editing.

Acknowledgment

This work was supported by Research Fund of the Sakarya University of Applied Sciences. Project Number: 2021-50-02-029.

References

- [1] Attarzadeh, N., *et al.*, New Promising Ceramic Coatings for Corrosion and Wear Protection of Steels: A Review, *Surfaces and Interfaces*, 23 (2021), Jan., 100997
- [2] Kordijazi, A., *et al.*, A Review of Application of Machine Learning in Design, Synthesis, and Characterization of Metal Matrix Composites: Current Status and Emerging Applications, *JOM*, 73 (2021), 7, pp. 2060-2074
- [3] VB, S., An Overview on the Preparation, Characterization and Properties of Electrodeposited-Metal Matrix Nanocomposites, *Nanosci. Technol. Open Access*, 1 (2014), 3, pp. 1-20
- [4] Mahidashti, Z., *et al.*, Review of Nickel-Based Electrodeposited Tribo-Coatings, *Trans. Indian Inst. Met.*, 71 (2018), 2, pp. 257-295
- [5] Li, H., *et al.*, Influence of Pulse Frequency on Corrosion Resistance and Mechanical Properties of Ni-W/B4C Composite Coatings, *Colloids Surfaces A Physicochem, Eng. Asp.*, 629 (2021), July, 127436
- [6] Zhang, Z., *et al.*, A Novel Synthesis Method for Functionally Graded Alloy Coatings by Induced Electrodeposition, *Mater. Lett.*, 312 (2022), April, 131681
- [7] Duru, E., *et al.*, Optimization of Ni-B Coating Bath and Effect of DMAB Concentration on Hardness and Wear, *Surfaces and Interfaces*, 22 (2021), Feb., 100880
- [8] Steffani, C., Meltzer, M., Electrodeposited Tungsten-Nickel-Boron: A Replacement for Hexavalent Chromium, Technical report, Lawrence Livermore Nat. Lab., Livermore, Cal., USA, 1995
- [9] Surdem, S., *et al.*, A Parametric Study on the Relationship between NaBH₄ and Tribological Properties in the Nickel-Boron Electroless Depositions, *Mater. Res. Express*, 6 (2019), 12, 125085
- [10] Makalesi, A., *et al.*, Akımsız Ni-P-W Kompozit Kaplamalarda PTFE Konsantrasyonunun Sertlik ve Asınma Uzerinde Etkisi, *Eur. J. Sci. Technol. Spec.*, 28 (2021), Nov., pp. 1356-1359
- [11] Hu, J., *et al.*, The Anticorrosive and Antifouling Properties of Ni-W-P-nSiO₂ Composite Coating in A Simulated Oilfield Environment, *Jom*, 70 (2018), 11 pp. 2619-2625
- [12] Huang, P. C., *et al.*, Preparation and Tribological Research of the Electrodeposited Ni[*sbn*]W Alloy Coatings for Piston Ring Application, *Surf. Coatings Technol.*, 411 (2021), Feb., 126980
- [13] Haseeb, A. S. M. A., *et al.*, Friction and Wear Characteristics of Electrodeposited Nanocrystalline Nickel-Tungsten Alloy Films, *Wear*, 264 (2008), 1-2, pp. 106-112

- [14] Szczygieł, B., Kołodziej, M., Composite Ni/Al₂O₃ Coatings and Their Corrosion Resistance, *Electrochim. Acta*, 50 (2005), 20, pp. 4188-4195
- [15] Ulu, S., et al., Characterization of TiO₂ Reinforced Electroless Ni-P-B-W-TiO₂ Multi Alloy Coatings: The Effect of TiO₂ Concentration, *Proceedings*, 19th International Metallurgy & Materials Congress, Istanbul, Turkey, 2018, pp. 1036-1039
- [16] Lajevardi, S. A., Shahrabi, T., Effects of Pulse Electrodeposition Parameters on the Properties of Ni-TiO₂ Nanocomposite Coatings, *Appl. Surf. Sci.*, 256 (2010), 22, pp. 6775-6781
- [17] Sadreddini, S., Afshar, A., Corrosion Resistance Enhancement of Ni-P-nanoSiO₂ Composite Coatings on Aluminum, *Appl. Surf. Sci.*, 303 (2014), June, pp. 125-130
- [18] Dogan, F., et al., Optimization of Pulsed Electro Co-Deposition for Ni-B-TiN Composites and the Variation of Tribological and Corrosion Behaviors, *Surf. Coatings Technol.*, 400 (2020), Oct., 126209
- [19] Chen, B., et al., Tribological Properties of Solid Lubricants (Graphite, h-BN) for Cu-Based P/M Friction Composites, *Tribol. Int.*, 41 (2008), 12, pp. 1145-1152
- [20] Dogan, F., et al., Tribology Study of Pulse Electrodeposited Ni-B-SWCNT Composite Coating, *Jom*, 74 (2022), 2, pp. 574-583
- [21] Duru, E., et al., Fabrication and Characterization of Graphene Oxide Reinforced NiB Composite Coating by Pulsed Electrodeposition Technique, *Diam. Relat. Mater.*, 120 (2021), Oct., 108688
- [22] Mohammadi, M., Ghorbani, M, Wear and Corrosion Properties of Electroless Nickel Composite Coatings with PTFE and/or MoS₂ Particles, *Journal Coatings Technol. Res.*, 8 (2011), 4, pp. 527-533
- [23] Safavi, M. S., et al., Electrodeposited Ni-Co Alloy-Particle Composite Coatings: A Comprehensive Review, *Surf. Coatings Technol.*, 382 (2020), Jan., 125153
- [24] Allahyarzadeh, M. H., et al., Structure and Wettability of Pulsed Electrodeposited Ni-W-Cu-(α -Alumina) Nanocomposite, *Surf. Coatings Technol.*, 307 (2016), Dec., pp. 525-533
- [25] Guglielmi, N., Kinetics of the Deposition of Inert Particles from Electrolytic Baths, *Journal Electrochem. Soc.*, 119 (1972), 8, 1009
- [26] Dogan, D., et al., Investigation of Mechanical and Tribological Characteristics of Ni-B Coatings Deposited on Steel, *Journal Boron*, 6 (2020), 1, pp. 209-215
- [27] Gultekin, D., et al., Improved Wear Behaviors of Lead-Free Electroless NiB and Ni-B/CeO₂ Composite Coatings, *Surf. Coatings Technol.*, 422 (2021), Sep., 127525
- [28] Urdem, S., et al., Evaluation of High Temperature Tribological Behavior of Electroless Deposited NiB-Al₂O₃ Coating, *Wear*, 482-483 (2021), May, 203960
- [29] Dogan, D., et al., Pulsed Electrodeposition of Ni-B/TiN Composites: Effect of Current Density on the Structure, Mechanical, Tribological, and Corrosion Properties, *Journal Asian Ceram. Soc.*, 8 (2020), 4, pp. 1271-1284
- [30] Gao, P., et al., Electrochemical Characteristics and Interfacial Contact Resistance of Ni-P/TiN/PTFE Coatings on Ti Bipolar Plates, *Journal Solid State Electrochem.*, 22 (2018), 7, pp. 1971-1981
- [31] Allahyarzadeh, M. H., et al., Mechanical Properties and Load Bearing Capability of Nanocrystalline Nickel-Tungsten Multilayered Coatings, *Surf. Coatings Technol.*, 386 (2020), Mar., 125472
- [32] Aslan, S., Duru, E., Microstructure and Wear Properties of Electrodeposited Ni-B-Al₂O₃ Composite Coating on Low Carbon Steel at Elevated Temperature, *Journal Mater. Eng. Perform.*, 31 (2022), Oct., pp. 1693-1704
- [33] Uysal, M., et al., Tribological Properties of Ni-W-TiO₂-GO Composites Produced by Ultrasonically-Assisted Pulse Electro Co-Deposition, *Surf. Coatings Technol.*, 410 (2021), Mar., 126942
- [34] Chen, L., et al., Effect of Surfactant on the Electrodeposition and Wear Resistance of Ni-Al₂O₃ Composite Coatings, *Mater. Sci. Eng. A*, 434 (2006), 1-2, pp. 319-325